



# Design of Dual Band and Tri-band Bandpass Filter (BPF) with Improved Inter-band Isolation Using DGS Integrated Coupled Microstrip Lines Structures

Sourav Moitra<sup>1</sup> · Ranjan Dey<sup>1</sup>

Published online: 16 October 2019  
© Springer Science+Business Media, LLC, part of Springer Nature 2019

## Abstract

A novel approach to design dual-band as well as a triple-band BPF with improved isolation is ventured in this paper. In dual-band filter, dual mode property of coupled line filters is utilized to obtain resonant frequencies at 2.4 GHz and 7.4 GHz suitable for WLAN and WiMAX application respectively. Additionally a rectangular-ring DGS element is introduced within the coupled line filter to obtain a separate mid-band resonance at 5.2 GHz. The frequency shifting property of the pass bands due to cross-coupling between the microstrip line resonators and the DGS element is mostly eliminated by implementing stepped impedance open stub (SIOS) technique. All filter configurations are fabricated, measured and compared with the simulated models to validate the practical effectiveness. Stop band isolation  $> 40$  dB and insertion loss (IL)  $< 0.8$  dB is attained in all the filter configurations.

**Keywords** Microstrip coupled line · Defected ground structure (DGS) · Stepped impedance open stub (SIOS) · Band pass filter (BPF)

## 1 Introduction

Multi-band band pass filter (BPF) is a major component in modern wireless communication system [1–5]. The existence of multi-band signals, especially in developed the wireless local area networks (WLANs) standards such as IEEE 802.11b (2.4 GHz), IEEE 802.11a (5.2 GHz) and also in WiMAX standard such as IEEE 802.16e (2.5 GHz) and in downlink of satellite communication system (7.4 GHz) has been growing with a fast pace. Recently, several approaches have been proposed to design dual band BPFs. Cascade connection of BPF and band stop filter are found to produce dual band pass response [6]. Dual-band BPF has also been proposed by combining two sets of resonators with common output and input [7]. An alternative approach using open interconnected split ring resonator (OISRR) has been successfully used to achieve UWB response in band pass filters [8]. Although dual band filters using distinct coupled line section are proposed where the width and gap are too small

---

✉ Sourav Moitra  
souravmoitra25@yahoo.in

<sup>1</sup> Department of Electronics and Communication Engineering, Dr. B C Roy Engineering College, Durgapur, West Bengal, India

(0.1–0.05 mm) which might be little tricky for the design engineers to control. Practically, this gap size ( $\leq 0.1$  mm) is critical during fabrication process in which high level of accuracy is essentially required [9].

Several methods to realize triple-band bandpass filters (BPFs) are also reported in recent past. Quendo et al. realized triple band BPF by using dual behavior resonators (DBRs) where each passband of the filter is separated by transmission zeros produced by the resonating of the open-stubs [10]. Stepped impedance resonators (SIRs) are also used to produce multiple transmission zeros and passbands [11]. However, the stopband characteristics of these filters still have some scope of improvement. An external impedance network is designed and inserted between the resonator and the input/output port to get the desired external quality factors [12]. Gap coupled structure can also be applied and the external quality factors can be modified to satisfy the requirements by simply changing the position of the feeding structures [13, 14].

In this paper, an approach to design a compact dual-band and a triple-band BPF with using coupled three line microstrip structure and a rectangular slotted DGS is presented. These filters are suitable for WiMAX, WLAN and satellite communication system oriented applications. A stepped-impedance open stub (SIOS) is used at the symmetrical plane of the filter to improve the higher passband selectivity and also to minimize the cross-coupling. Proposed multiband filters exhibits low insertion loss, good passband selectivity, and wide rejection level of the stopband.

## 2 Filter Design Methodology

Design of proposed multiband filters are accomplished by using coupled microstrip line structures and a rectangular DGS feeded with stepped microstrip lines. Proposed filters are designed and fabricated on Neltec NH9320 substrate having a thickness ( $h$ ) of 30 mils with dielectric constant ( $\epsilon_r$ ) of 3.2 and 0.0024 loss tangent ( $\tan\delta$ ). A pair of stepped down microstrip feedlines are used for excitation purpose in the proposed filter configurations. With variation of the gap width ‘S’, intensity of edge coupling between two feed lines can be tuned. The  $50\ \Omega$  feed lines are designed by using the following relations for proper impedance matching.

$$\epsilon_{\text{reff}} = \frac{\epsilon_r + 1}{2} + \frac{\epsilon_r - 1}{2}(1 + 10h/B)^{-1/2}$$

$$Z_0 = \frac{119.9}{\sqrt{2(\epsilon_r + 1)}} \left[ \ln \left( 4 \frac{h}{B} + \sqrt{16(h/B)^2 + 2} \right) - \frac{1}{2} \left( \frac{\epsilon_r - 1}{\epsilon_r + 1} \right) \left( \ln \frac{\pi}{2} + \frac{1}{\epsilon_r} \ln \frac{4}{\pi} \right) \right]$$

where ‘ $h$ ’, ‘ $B$ ’, ‘ $\epsilon_r$ ’ and ‘ $Z_0$ ’ represents the substrate thickness, width of feed lines, dielectric constant of the substrate and the characteristic impedance of feed lines respectively (Table 1). Figure 1a shows the microstrip coupled line open-ended feed whereas the equivalent circuit is shown in Fig. 1b.

### 2.1 Single Band DGS Integrated BPF

Defected Ground Structures (DGS) are often employed to obtain band pass response in microstrip filters. Properties of DGS structures are investigated which is shown to exhibit wide stopband as well as greater Q-factor in Microstrip filters [15, 16]. These structures

**Table 1** Dimensions of open ended microstrip feedlines

Parameters	F	B	$L_f$	$W_f$	S
Dimension (mm)	10	1.93	18.45	1	0.1

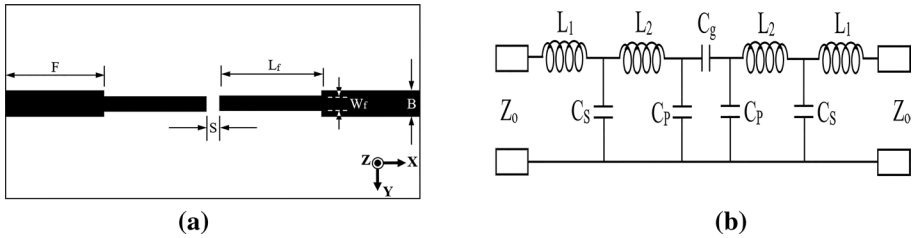


**Fig. 1** **a** Open-ended microstrip feed lines and **b** equivalent circuit

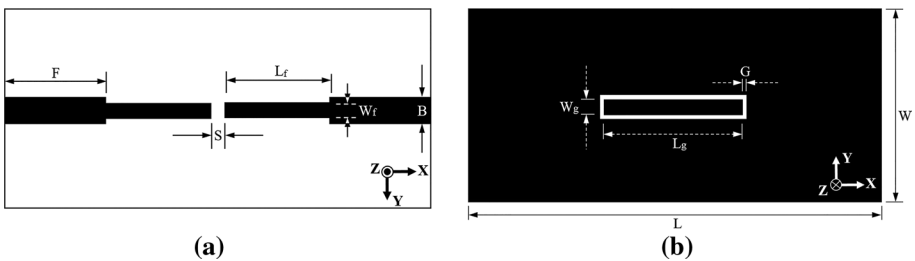


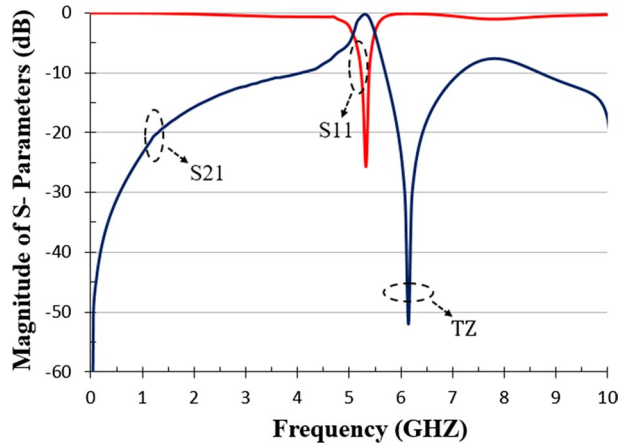
**Fig. 2** Design layout of DGS integrated single band microstrip BPF **a** top and **b** bottom

are also used to obtain dual and tri-band response [17, 18]. Several DGS configurations are reported which enables engineers to design filter design with higher degree of stopband rejections and isolation [19–21]. A rectangular ring shaped DGS elemental structure is used in the present study. Important parameters such as  $L_g$ ,  $G$  and  $W_g$  effectively control the equivalent inductance as well the DGS capacitance for which the center frequency of the passband resonance can be varied as per application requirements. Small changes in these parameters are found to have an impact of the lower and higher cut-off of the transmission passband. The schematic representation of the DGS integrated BPF is shown in Fig. 2, while the S-parameter results are depicted in Fig. 3. The pass band resonance is obtained at 5.2 GHz with insertion loss (IL) < 0.6 dB is achieved. Dimensions of the filter layout are given in Table 3.

**2.2 Dual Band Microstrip Coupled Line BPF**

Coupled line structures are widely used to design multiband filters for its simple design as well as straightforward fabrication technique. Simple sections of microstrip lines are used to form these coupled line structures. These coupled line structures works on the principle of even and odd modes. With analysing these two modes, coupled line structures can be used to design a suitable multiband filter. A clear representation of odd and even modes presented in a coupled line structure are shown in Fig. 4a, b respectively.

**Fig. 3** S-parameters of DGS integrated single band microstrip BPF



The characteristic modes for a symmetric parallel-coupled line structures are odd- and even-modes, and the image impedance is derived as [15]:

$$Z_{is} = \sqrt{\left[ csc^2 \theta_C (Z_{0e} - Z_{0o})^2 - cot^2 \theta_C (Z_{0e} + Z_{0o})^2 \right]}$$

where  $\theta_C$  is defined as the electric length of the parallel-coupled line, and  $Z_{0e}$  and  $Z_{0o}$  are defined as the characteristic impedances of the even- and odd-modes, respectively. As the asymmetric parallel-coupled line structure is adopted, the characteristic modes are represents c- and  $\pi$ -modes [16]. However for asymmetric parallel-coupled structure and the image impedance function can be expressed as [15]:

$$Z_{ia} = \frac{1}{2} \sqrt{\left[ csc^2 \theta_C (Z_{0c} - Z_{0\pi})^2 - cot^2 \theta_C (Z_{0c} + Z_{0\pi})^2 \right]}$$

where  $\theta_C$  is defined as the electric length of the asymmetric parallel-coupled line, and  $Z_{0c}$  and  $Z_{0\pi}$  are defined as the characteristic impedances of the c and  $\pi$ -modes, respectively.

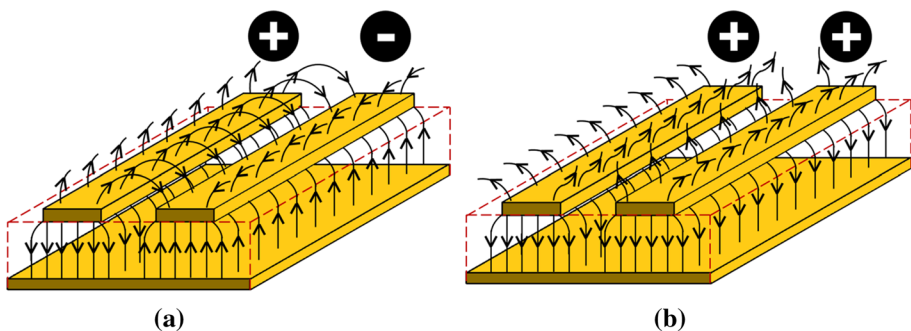


**Fig. 4** **a** Odd mode E-field pattern of parallel microstrip coupled line; **b** even mode E-field pattern of microstrip coupled line

Based on the above operational principles of Microstrip lines several methods of designing band pass filters are discussed and presented in recent past. A dual wideband bandpass filters with internally coupled microstrip lines is presented [22]. Good out of band rejection for  $\approx 1$  GHz is achieved by this technique. Effect of multiple capacitively loaded coupled lines are studied which also shows band filter response with improved stopband isolation [23]. Another technique is to use quarter wavelength coupled lines which have the property to produce wideband response in differential filter circuits [24]. Ultra wide band response in band pass filters can also be achieved by the help of three coupled line microstrip structures [25]. Although these methods presents some excellent ideas, further insight in multi-band BPF designs happens to be a lucrative area as there is still a vast scope to improve filter properties and practical application oriented designs. Proposed coupled line filters presented in this paper are loaded with single and double microstrip lines which work as dual band BPFs. Figure 5a, b represents top view of our proposed filter layouts. It may be noted that the ground plane of both structures are kept unperturbed in these cases. Whereas Fig. 5c, d defines the coupling schemes generated for asymmetric and symmetric coupled line structures respectively. These two coupling matrix are responsible for the formation of the lower passbands (2.4 GHz) of proposed filters. Figure 5e represents the coupling matrix generated for the edge coupling of the proposed stepped down feed lines. This coupling matrix is responsible for the generation of upper side passbands ( $\approx 7.4$  GHz). Fabricated prototypes of proposed filters are shown in Fig. 6a–d. Comparisons between the simulated and measured results for both single and double microstrip line loaded filters are shown in Figs. 7 and 8 respectively.

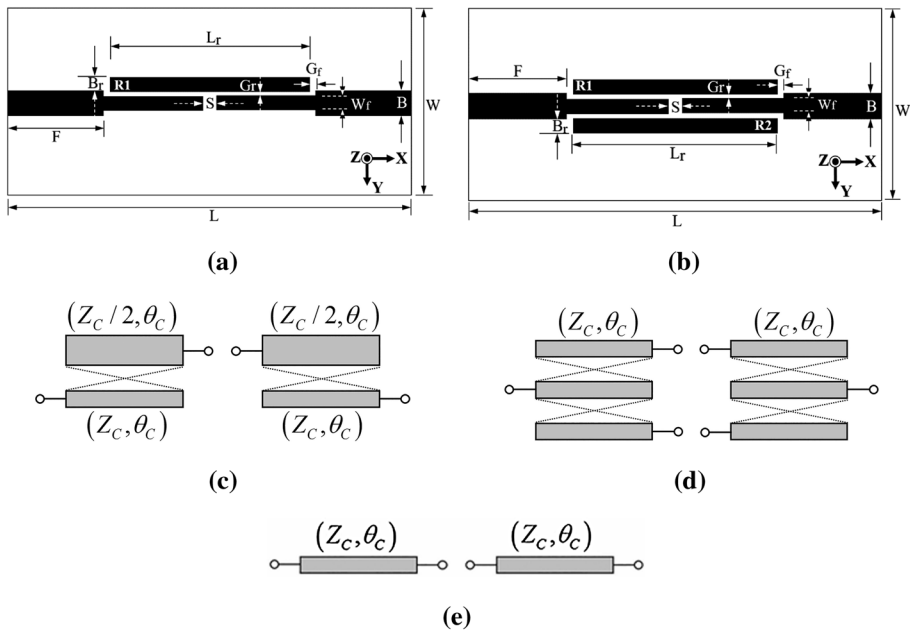


**Fig. 5** Schematic diagram of the top layer of **a** single microstrip line resonator loaded BPF and **b** dual microstrip line resonator loaded BPF; equivalent circuit of **c** asymmetric parallel-coupled line structure at 2.4 GHz, **d** symmetric parallel-coupled three line structure at 2.4 GHz and **e** proposed coupled line filter structure at 7 GHz

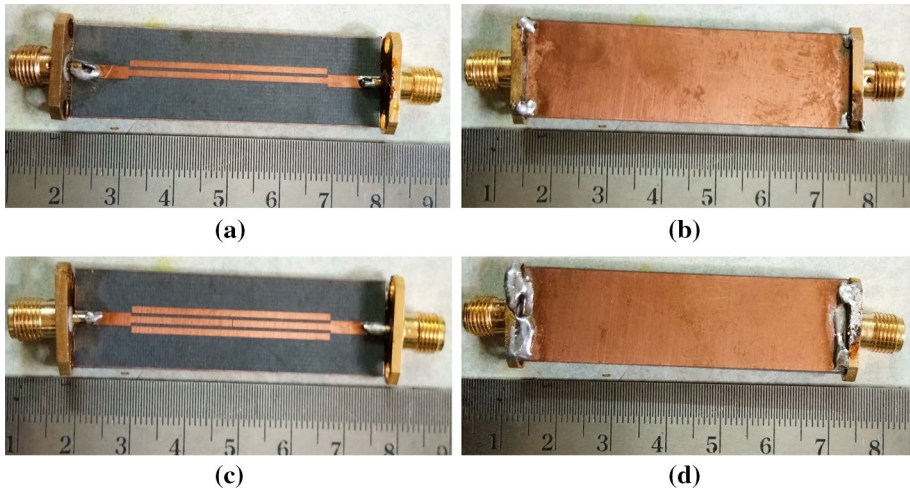
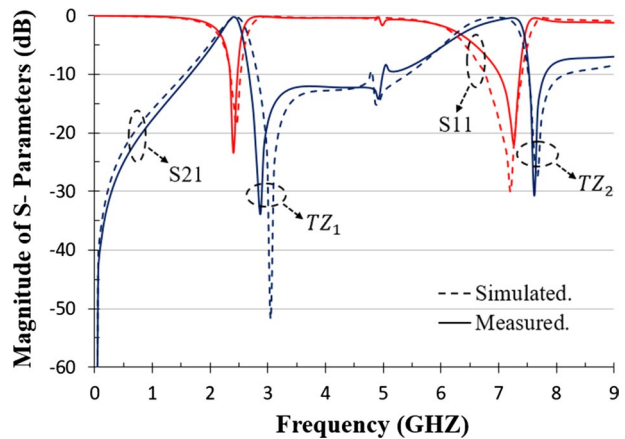


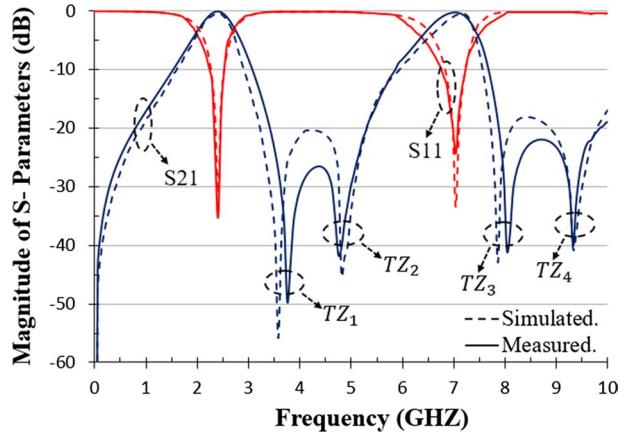
**Fig. 6** Fabricated prototypes of single microstrip line resonator loaded BPF **a** top and **b** bottom and dual microstrip line resonator loaded BPF **c** top and **d** bottom

**Fig. 7** Comparison of simulated and measured S-parameters of single microstrip line resonator (R1) loaded BPF



The number of transmission zeroes within the intermediate frequencies is directly related to the number of resonators used. It has been observed that by using both schemes (single microstrip resonator and dual microstrip resonator), dual band response has been achieved. However for dual resonant structure, the stopband isolation between successive passbands is largely improved. Close to 20 dB isolation has been achieved by using this technique. It is to be noted that further isolation of higher frequencies beyond the second passband are also achieved by using dual Microstrip resonator circuits. Other important filter parameters as obtained by comparing the simulated and the measured results are given in Table 2.

**Fig. 8** Comparison of simulated and measured S-parameters of dual microstrip line resonator (R1 + R2) loaded BPF



### 2.3 DGS and Microstrip Coupled Line Integrated Triple Band BPF

The formation of triple band response by integrating the rectangular ring DGS and Microstrip coupled lines is discussed in this section. As discussed in the previous sections, the DGS slot is responsible for producing a narrow passband at 5.2 GHz while dual passbands at 2.4 GHz and 7.4 GHz are obtained by using microstrip coupled line structures. To obtain passbands at all of these frequencies simultaneously within the same structure, these two structures are merged together. Conditional adjustments are performed to preserve important filter characteristics like intermediate isolation between successive passbands and insertion loss. Return loss  $\approx 30$  dB is achieved in almost all passbands by using single resonant coupled line section (R1) and DGS. Likewise improved RL  $\approx 40$  dB is attained by using double such lines (R1 + R2) coupled with the DGS structure. Insertion loss  $\leq 0.5$  dB is achieved in all the three passbands. Figure 9 represents the structural layouts of the DGS integrated coupled line BPF whereas fabricated prototypes of both filter configurations are shown in Fig. 10a–d. The S-parameter of DGS integrated single resonant coupled line is depicted in Fig. 11 whereas the field coupling of the double couple line DGS integrated filter and the S-parameter can be observed in Figs. 12 and 13 respectively.

Integration of the DGS elements in both coupled line filters confirms that the mid-band frequency of the three band remains same but resonant frequencies of the other two bands experience a slight shift towards the higher spectrum. This results mainly due to the cross coupling between the microstrip line resonators and the DGS structure which was not predominant in

**Table 2** Performance datasheet of dual-band BPFs

Parameters	1st band	2nd band	1st band	2nd band
	For R1 only	For R1 only	For R1 + R2	For R1 + R2
Resonant frequency (GHz)	2.4	7.4	2.4	7.3
Insertion loss (dB)	0.17	0.34	0.19	0.28
Return loss (dB)	24	30	35	33.5
Transmission B.W (MHz)	212	410	258	397



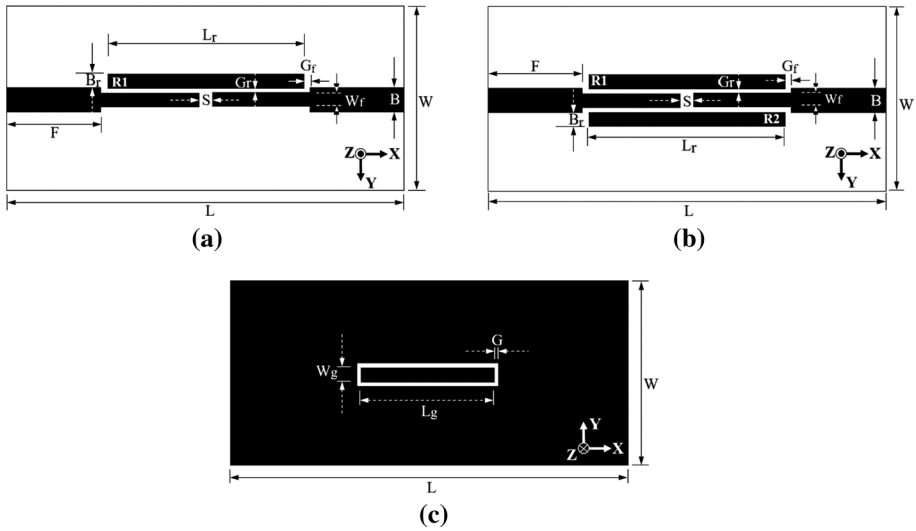


**Fig. 9** a Schematic diagram DGS integrated single microstrip line resonator BPF b DGS integrated double microstrip line resonator BPF and c ground plane of both BPF configurations

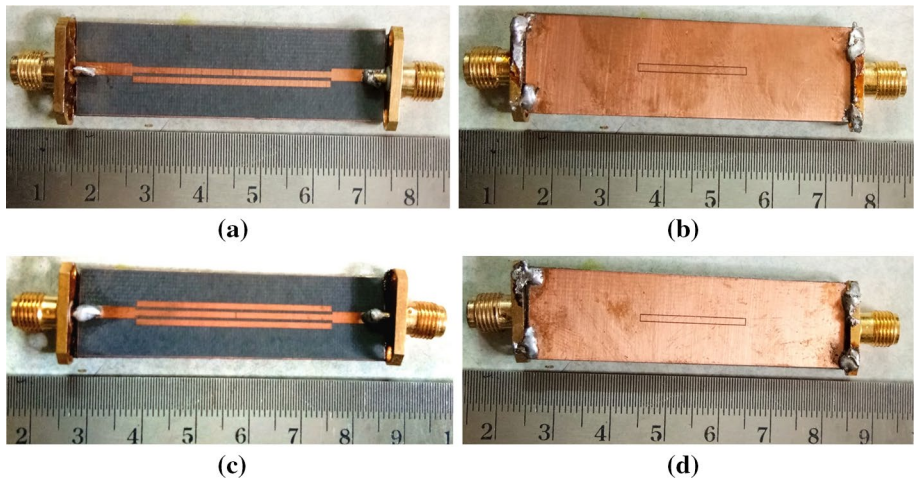


**Fig. 10** Fabricated prototypes of DGS integrated single microstrip line resonator BPF a top and b bottom and fabricated prototypes of DGS integrated double microstrip line resonator BPF c top and d bottom

absence of rectangular DGS structure. Resonant frequencies of first and third band depend on the electric length of the microstrip line resonators and open-ended microstrip feed lines respectively. However the resonant frequency of the mid-band is a function of the electrical length of the rectangular ring DGS structure. For the single microstrip line resonator loaded filter resonant frequency of 1st band and 3rd band are found to shift by 0.1 GHz and 0.5 GHz respectively towards higher spectrum. In other case for the double microstrip line resonator loaded filter resonant frequency of 1st band and 3rd band will be shifted by 0.1 GHz and



**Fig. 11** S-parameters of DGS integrated single microstrip line resonator BPF (R1 + DGS)

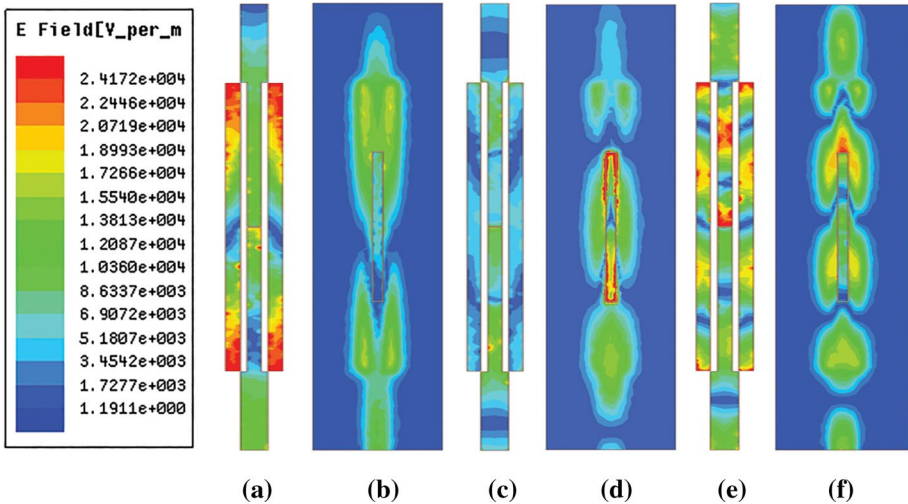
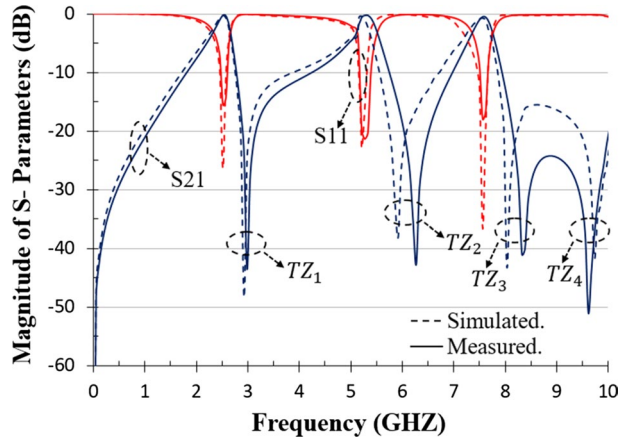


**Fig. 12** Simulated electric field distribution of DGS integrated double microstrip line resonator BPF (R1 + R2 + DGS) at **a** top at 2.5 GHz, **b** bottom at 2.5 GHz, **c** top at 5.2 GHz, **d** bottom at 5.2 GHz, **e** top at 7.4 GHz and **f** bottom at 7.4 GHz

0.4 GHz respectively. Coupled three microstrip-line filter with DGS exhibits all band-pass characteristics of a triple-band BPF keeping all important behavior suitable for practical applications. The dimensional variables of all filter configurations are given in Table 3 whereas Table 4 provides performance datasheet of the triple band BPF.

**Fig. 13** S-parameters of DGS integrated double microstrip line resonator BPF (R1 + R2 + DGS)

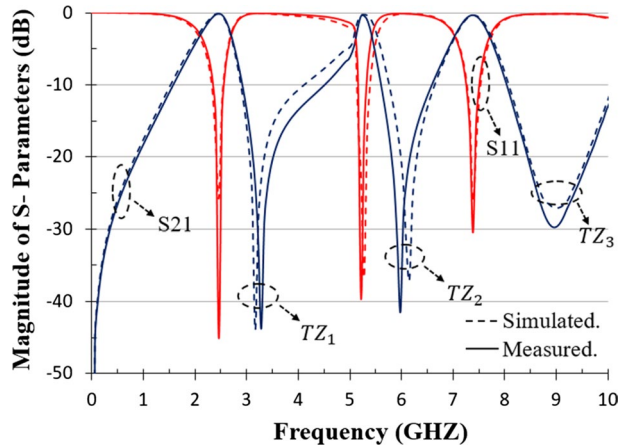


**Table 3** Major dimensions of all filter configurations

Filter configuration	Variables (mm)												
	F	B	L <sub>f</sub>	W <sub>f</sub>	L <sub>r</sub>	B <sub>r</sub>	G <sub>r</sub>	G <sub>f</sub>	S	h	L <sub>g</sub>	W <sub>g</sub>	G
DGS loaded filter	10	1.93	18.45	1	–	–	–	–	0.1	0.8	19	1	0.1
coupled line filter	10	1.93	18.45	1	36.8	1	0.465	0.1	0.1	0.8	–	–	–
DGS loaded coupled line filter	10	1.93	18.45	1	36.8	1	0.465	0.1	0.1	0.8	19	1	0.1

**Table 4** Performance datasheet of triple-band BPF design specifications

Filter specification	1st band		2nd band		3rd band	
	R1 + DGS	R1 + R2 + DGS	R1 + DGS	R1 + R2 + DGS	R1 + DGS	R1 + R2 + DGS
Resonant frequency (GHz)	2.5	2.5	5.2	5.2	7.5	7.4
Insertion loss (dB)	0.35	0.12	0.31	0.43	0.54	0.33
Return loss (dB)	15.5	45.1	21.3	39.7	17.9	30.5
Transmission B.W (MHz)	125	219	208	180	155.5	257

### 3 Conclusion

Simple and effective methodology to design single, dual and triple band BPF is proposed in this paper. Initially a rectangular ring shaped Defected Ground Structure (DGS) slot is used to obtain single narrow passband  $\approx 5.2$  GHz suitable for WLANs. Microstrip coupled line structures are used separately to design a dual band BPF operating in WLAN 2.4 GHz and WiMAX 7.4 GHz. The two filter configurations are integrated together successfully resulting in a triple band response with eminent insertion loss and isolation performances. The key contribution of this paper is the attainment of all application oriented transmission

bands with improved isolation between the adjacent passband frequencies. Moreover pass-band frequencies and band width of all three bands can be controlled as per application requirements.

## References

1. Mo, S.-G., Yu, Z.-Y., & Zhang, L. (2009). Design of triple-mode bandpass filter using improved hexagonal loop resonator. *Progress in Electromagnetics Research*, *96*, 117–125.
2. Coudos, S. K., Zaharis, Z. D., & Yioultis, T. V. (2010). Application of a differential evolution algorithm with strategy adaptation to the design of multi-band microwave filters for wireless communications. *Progress in Electromagnetics Research*, *109*, 123–137.
3. Wu, L.-S., Mao, J.-F., Shen, W., & Yin, W.-Y. (2010). Extended doublet bandpass filters implemented with microstrip resonator and full-/half-mode substrate integrated cavities. *Progress in Electromagnetics Research*, *108*, 433–447.
4. Chiou, Y.-C., Yang, P.-S., Kuo, J.-T., & Wu, C.-Y. (2010). Transmission zero design graph for dual-mode dual-band filter with periodic stepped-impedance ring resonator. *Progress in Electromagnetics Research*, *108*, 23–36.
5. Wu, H.-W., Liu, S.-K., Weng, M.-H., & Hung, C.-H. (2010). Compact microstrip bandpass filter with multipurious suppression. *Progress in Electromagnetics Research*, *107*, 21–30.
6. Tsai, L. C., & Hsue, C. W. (2004). Dual-band bandpass filters using equallength coupled-serial-shunted lines and Z-transform technique. *IEEE Transactions on Microwave Theory and Techniques*, *52*(4), 1111–1117.
7. Chen, C., & Hsu, C. (2006). A simple and effective method for microstrip dual-band filters design. *IEEE Microwave and Wireless Components Letters*, *16*(5), 246–248.
8. Hinojosa, J., Martinez-Viviente, F. L., de Dios Ruiz, J., Alvarez-Melcon, A. (2015). Modified split-ring resonator for microstrip dual-band notch filter. In *Microwave conference (EuMC), 2015 European* (pp. 813–816), 7–10 September 2015.
9. Singh, P. K., Basu, S., & Wang, Y. H. (2007). Planar ultra-wideband bandpass filter using edge couple microstrip lines and stepped impedance open stub. *Microwave Wireless Component Letters*, *17*(9), 649–651.
10. Quendo, C., Rius, E., Manchec, A., Clavet, Y., Potelon, B., Favennec, J.-F., & Person, C. (2005). Planar tri-band filter based on dual behavior resonator. In *European microwave conference 2005, Paris, France* (pp. 269–272).
11. Huang, J.-F., & Hsu, M.-H. (2005). Design and implement of high performance and miniaturization of SIR microstrip multi-band filters. *IEICE Transactions on Electronics*, *7*, 1420–1429.
12. Kuo, J. T., & Cheng, H. S. (2004). Design of quasi-elliptic function filters with a dual-passband response. *IEEE Microwave and Wireless Components Letters*, *14*, 472–474.
13. Sun, S., & Zhu, L. (2005). Compact dual-band microstrip bandpass filter without external feeds. *IEEE Microwave and Wireless Components Letters*, *15*, 644–646.
14. Chen, C.-Y., & Hsu, C.-Y. (2006). A simple and effective method for microstrip dual-band filters design. *IEEE Microwave and Wireless Components Letters*, *16*, 246–248.
15. Park, J. S., Yun, J. S., & Ahn, D. (2002). A design of the novel coupled line bandpass filter using defected ground structure with wide stopband performance. *IEEE Transactions on Microwave Theory and Tech.*, *50*(09), 2037–2043.
16. Woo, D. J., Lee, T. K., Lee, J. W., Pyo, C. S., & Choi, W. K. (2006). Novel U-slot and V-slot DGSs for bandstop filter with improved Q-factor. *IEEE Transactions on Microwave Theory and Tech.*, *54*(06), 2840–2847.
17. Ren, L. Y. (2010). Tri-band bandpass filters based on dual plane microstrip/DGS slot structure. *IEEE Microwave and Wireless Component Letters*, *20*(08), 429–431.
18. Song, Y., Yang, G. M., & Geyi, W. (2014). Compact UWB bandpass filter with dual notched bands using defected ground structures. *IEEE Microwave and Wireless Component Letters*, *24*(04), 230–232.
19. Rahman, A. A., Verma, A. K., Boutejdar, A., & Omar, A. S. (2004). Compact stub type microstrip bandpass filter using defected ground plane. *IEEE Microwave Wireless Component Letters*, *14*(04), 136–138.
20. Park, J. S., Yun, J. S., & Park, C. S. (2007). DGS resonator with interdigital capacitor and application to bandpass filter design. *IET Electronics Letters*, *40*(07), 433–434.

21. Ren, L. Y., & He, H. (2009). Wide stopband bandpass filter based on dual plane microstrip/interdigital DGS slot structure. *IET Electronics Letters*, 45(25), 1331–1332.
22. Zhang, R., & Zhu, L. (2014). Synthesis and design of dual wideband bandpass filters with internally coupled microstrip lines. *IET Microwave Antennas and Propagation*, 08(08), 556–563.
23. Tang, C. W. (2007). Design of a microstrip filter using multiple capacitively loaded coupled lines. *IET Microwave Antennas and Propagation*, 01(03), 651–657.
24. Feng, W., & Che, W. (2016). Compact wideband differential filter using quarter wavelength coupled lines. *Journal of Electromagnetic Waves and Applications*, 30(11), 1381–1390.
25. Weng, M. H., Huang, C. Y., Hung, C. Y., & Lan, S. W. (2012). Design of a ultrawideband bandpass filter by using coupled three line microstrip structure. *Journal of Electromagnetic Waves and Applications*, 26(05), 716–728.

**Publisher's Note** Springer Nature remains neutral with regard to jurisdictional claims in published maps and institutional affiliations.



**Sourav Moitra** received his B.Tech. (Electronics and Communication Engineering) in 2005 from the West Bengal University of Technology. He was associated with several electronics industries in between 2005 and 2007. He received his M.Tech. (Microwave Engineering) in 2009 from The University of Burdwan. He has been associated with Dept. of Atomic Energy, Govt. of India on a project related to the development of high power RF tubes. At present he is associated with Dr. B. C. Roy Engineering College, Durgapur, India as Assistant Professor in the Dept. of Electronics and Communication Engineering. He has several publications in International Journals and Conferences. His current research interest includes design and development of microwave and millimeter wave passive circuits based on microstrip line and substrate integrated waveguides applicable in wireless networks.



**Ranjan Dey** obtained his B.Tech. degree in Electronics and Communication Engineering from Maulana Abul Kalam Azad University of Technology, Kolkata, India in 2017. He has authored several papers in national and international conferences. His current research includes design of microwave and millimeter-wave passive components based on Microstrip line, SIWs and Metamaterials.